

We are IntechOpen, the world's leading publisher of Open Access books Built by scientists, for scientists

6,900

Open access books available

185,000

International authors and editors

200M

Downloads

Our authors are among the

154

Countries delivered to

TOP 1%

most cited scientists

12.2%

Contributors from top 500 universities



WEB OF SCIENCE™

Selection of our books indexed in the Book Citation Index
in Web of Science™ Core Collection (BKCI)

Interested in publishing with us?
Contact book.department@intechopen.com

Numbers displayed above are based on latest data collected.
For more information visit www.intechopen.com



Precision Improvement in Inertial Miniaturized Navigators Based on Fuzzy Logic Denoising of Sensors Signals

Teodor Lucian Grigorie and
Ruxandra Mihaela Botez

Additional information is available at the end of the chapter

<http://dx.doi.org/10.5772/67966>

Abstract

The chapter presents a new strategy to improve the precision of the inertial navigators processing in a fuzzy manner the signals provided by the miniaturized sensors equipping their inertial measurement units (IMU). To apply the developed technique, the hardware component of the inertial measurement units was specifically designed to include some redundant clusters of inertial sensors disposed in linear configurations on the measurement axes. The algorithm acts at the level of each detection cluster designed to measure an acceleration or angular speed along with an IMU axis by fusing the data obtained from the sensors in respective cluster. Based on the standard deviations of the sensors signals estimated for a data frame with a well-known size, the fuzzy logic mechanism provides a set of weights associated with each sensor in cluster, which are further used to fuse the data acquired from sensors at the current time. The algorithm has an adaptive character, the data frame used to estimate the standard deviations of the sensors signals being permanently updated with the new sensors measurements, and, in this way, the weights associated with each sensor are reestimated at each measurement step.

Keywords: inertial navigation, miniaturized sensors, data fusion, fuzzy logic, redundant configurations, noise reduction, precision improvement

1. Introduction

The permanent change at the level of the sensor fabrication technologies in the last two decades aiming especially toward miniaturization produced a significant change in the navigation and

positioning systems field from the point of view of strap-down inertial navigation systems (SDINS). Therefore, more and more applications have been developed and are currently developed starting from this concept and based on miniaturized inertial measurement units and miniaturized data processing systems. These new technologies, MEMS (micro-electro-mechanical systems), NEMS (nano-electro-mechanical systems), MOEMS (micro-opto-electro-mechanical systems), or NOEMS (nano-opto-electro-mechanical systems), are currently successfully applied in the inertial sensors, dedicated to a large part of the SDINS applications. Actually, due to the miniaturization, the SDINS systems application field has been seriously extended beyond the classical navigation systems equipping the vehicles in the aerospace industry, at the level of land-vehicle applications, robotics, medicine, and assisted living [1–4]. The distribution of the inertial sensor fabrication technologies on future applications accuracy classes can be organized as in **Figure 1** [1]. It can be easily observed that the accuracy level for NEMS technologies (possibly NOEMS) are still at the commercial applications level; IOG—integrated optics gyro, IFOG—interferometric fiber optic gyro, HRG—hemispherical resonant gyro, PCF-FOG—photonic crystal fiber-fiber optic gyro.

Included in the dead-reckoning navigation systems category, the SDINS was succeeded on the market due to its availability to provide the vehicle speed and position with abundant dynamic information, due to the possibility to calculate at an extremely high rate comparatively with the GPS system, and due to its excellent short-term performance. Having

<i>Very Precise Navigation</i>	<i>Long-Range Guidance</i>	<i>1 nm/hr Navigator</i>	<i>Tactical Weapons</i>	<i>Comercial Consumer</i>
Accelerometer Technology				
Cold Atom	Cold Atom	MEMS	MEMS	MEMS
Mechanical	MEMS			
	Mechanical			NEMS
Gyro Technology				
Cold Atom	Cold Atom	IOG	MEMS	MEMS
IFOG	IFOG			
	HRG	PCF FOG		NEMS
	IOG			

Figure 1. Inertial sensor technologies on the application accuracy classes.

characteristics complementary to satellite positioning systems, in time, it became an important component of the modern navigation systems near the GPS [5–6]. If the two systems are used in an integrated configuration, for a short time, derived from the quality of the used inertial sensors, the inertial navigator can overcome the nonavailability of GPS signals and can maintain in this way the navigation solution at a high quality; a well-designed INS/GPS navigator provides improved performance in terms of accuracy, availability, and reliability in front of a simple GPS system.

From another point of view, the inertial navigators are subjected to various error sources, their main deficiency residing in the great accuracy degradation over time mainly due to the quality of the used inertial sensors [7–9]. New miniaturization technologies plays an important role in the reduction of the cost and the volume of the inertial sensors, which, apparently, offers an important advantage for the miniaturized inertial sensors, but, in fact, the fabrication processes of such sensors make these very sensitive to the changes of the environmental conditions: temperature, pressure, electric and magnetic fields, and vibrations. Therefore, the sensors output can vary quickly, widely, and sometimes randomly and is very hard to be modeled. In many cases, this sensitivity leads to the decreased sensor performance, adding more error types, and possibly, with higher values than those of classical sensors [3, 9].

In this context, the need to develop low-cost, small-size, and high-precision INS/GPS integrated navigators, which are able to be used also in GPS challenging environments, generated few research directions in the field; the main two being [4–6, 10–14]: (1) to develop standalone accurate SDINS structures with miniaturized IMUs; (2) to develop new INS/GPS data-fusion methods based on artificial intelligence algorithms, having objectives to overcome the limitations in terms of model dependency, prior knowledge dependency, and linearization dependency.

The increase of the SDINS accuracy in standalone configuration targets, in fact, the improvement of the quality for the signals provided by the IMUs to the navigation processor through the obtaining of high quality miniaturized sensors or through the development of various IMU hardware architectures accompanied by right numerical algorithms able to produce sensor errors estimation and compensation [9, 13, 14]. Two categories of errors parasitize the inertial sensors: deterministic errors and stochastic errors. For the deterministic errors, the specialists conceived various calibration procedures, which can easily estimate and eliminate it. Unfortunately, the stochastic error estimation necessitates a more complex process and they cannot be fully removed from the sensors data. For both categories of inertial sensors (accelerometers and gyros), the most important stochastic errors are caused by noise and by instability of bias and of scale factor [7].

The main difficulty with the noise is related to the impossibility to apply a direct filtering procedure by using classical methods, because, in terms of frequency spectrum, it is superimposed on the band 0–100 Hz of the navigation useful signal [7]. As a consequence, many researches have been initiated to find alternative solutions to limit its impact on the solution of navigation. On the other way, it must not forget that at the level of the noise there are present two components, long term noise (low frequency noise) and short term noise (high frequency noise), each one with its own spectral characteristics and with its own compensation mechanism: optimal low pass filtering or using algorithms that fusing the data from multiple sensors [13, 15–19].

Our identified way to improve the quality of the inertial sensor signals is based on the use of redundant detection clusters with the sensors disposed in linear configurations along each detection axis in IMU (**Figure 2**) [9, 13]. For each cluster, the measured data are subsequently fused to provide to the navigation processor a better measured signal of acceleration or angular speed for the respective axis in IMU. Simultaneously, this structure provides the advantage to have a redundant inertial navigator in terms of the detection unit components, i.e., when one or more sensors in a detection cluster break down they are removed from calculation process but the system still remains operational. The inertial sensors in the same cluster have the sensitivity axes parallel and oriented in the same sense with the detection axis.

The proposed fuzzy logic procedure was mainly designed to produce effects at the level of the sensor noise, but some benefits were also noted at the level of bias effects reduction.

The work exposed here is related to a research project developed in Romania and financed by the Executive Unit for the Financing of Higher Education and University of Scientific Research, which aimed at the strap-down inertial navigators' precision improvement by using redundant sensor networks for their IMUs and new adaptive numerical algorithms for data fusion.

In this chapter, the information is structured as follows: Section 1 is constituted by a short introduction; Section 2 exposes the algorithm basic elements and structure, including the fuzzy logic mechanism; Section 3 shows the numerical simulation results obtained with the developed algorithm for detection clusters with various sizes and sensors types; Section 4 provides the results obtained with some experimental data acquired with detection clusters with six MEMS sensors each (assisted by an integrated GPS/INS navigator as reference positioning system) and processed for a bidimensional INS navigator; and Section 5 highlights the benefits brought by the algorithm in the form of the conclusions.

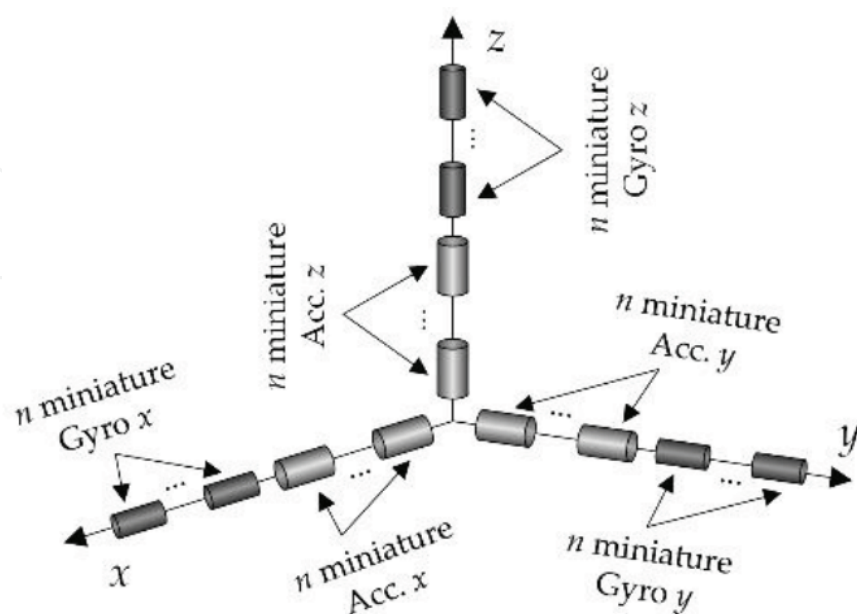


Figure 2. Inertial sensors disposed in linear configurations along each detection axis in IMU.

2. Data fusion algorithm basic elements and structure

To describe the generalized form of the proposed algorithm, it is denoted with n the number of collinear sensors included in a detection cluster, as in **Figure 2**. On the other way, if x_i ($i = 1 \div n$) are the measurements of the x quantity provided by the n sensors, characterized by the standard deviations σ_i ($i = 1 \div n$), then the weighted mean obtained by applying the data fusion algorithm conducts to the x_e estimate of the x quantity under the next form [14]:

$$x_e = w_1 \cdot x_1 + w_2 \cdot x_2 + \dots + w_n \cdot x_n = \sum_{i=1}^n w_i \cdot x_i \quad \left(\sum_{i=1}^n w_i = 1 \right); \quad (1)$$

w_i ($i = 1 \div n$) are the weights of the x_i ($i = 1 \div n$) measurements. For each sensor, the standard deviation is evaluated starting from the last m samples acquired from it. The algorithm has an adaptive character, the data frame used to estimate the standard deviations of the sensors signals being permanently updated with the new sensor measurements, and, in this way, the weights associated with each sensor are reestimated at each measurement step. The estimation of the new weight set is realized based on a fuzzy logic mechanism. The necessary data frame used in the estimation of sensors standard deviations is built using a FIFO (first in first out) buffer with n channels and able to memorize m successive samples on each channel. In this way, at each measurement time, the last column in the data frame goes out from the buffer and a new one comes in; two consecutive data frames are superposed with $(m - 1)$ samples [13]. The standard deviations of the n -independent channels result with the next equation [13, 14]:

$$\sigma_i(k) = \sqrt{\frac{1}{m} \sum_{j=1}^m [x_i(j) - \bar{x}_i(k)]^2}, \quad (i = \overline{1, n}); \quad (2)$$

$x_i(j)$ is the j th measurement provided by the i th sensor in the k th data frame; $\sigma_i(k)$ is the standard deviation for the k th data frame, which characterize the i th sensor; and $\bar{x}_i(k)$ is the arithmetic mean of the i th sensor data for the k th data frame [14]. The value of $\sigma_i(k)$ is used to fuse the data at the next sensor reading.

According to the proposed algorithm, a fuzzy logic controller is used in each channel of a detection cluster, and, based on the standard deviation, $\sigma_i(k)$ of the m consecutive samples acquired from the sensor in the k th data frame provides a weight $w_i^{\text{fuzzy}}(k)$ ($i = \overline{1, n}$) for the respective sensor. Based on the fact that in a weighted sum, the sum of all parts weight should be equal to 1, the sensors weights are recalculated and result with the equations [13, 14]):

$$w_1(k) = \frac{w_1^{\text{fuzzy}}(k)}{\sum_{i=1}^n w_i^{\text{fuzzy}}(k)}, \dots, w_n(k) = \frac{w_n^{\text{fuzzy}}(k)}{\sum_{i=1}^n w_i^{\text{fuzzy}}(k)}. \quad (3)$$

As a consequence, by calculating the weighted sum from the data fusion equation, at the time t_{k+1} , the x_e estimate of x is [13, 14]:

$$x_e(k+1) = w_1(k) \cdot x_1(k+1) + w_2(k) \cdot x_2(k+1) + \dots + w_n(k) \cdot x_n(k+1), \quad (4)$$

i.e.,

$$x_e(k+1) = \sum_{i=1}^n w_i(k) \cdot x_i(k+1), \quad \left(\sum_{i=1}^n w_i(k) = 1 \right). \quad (5)$$

Based on the previous considerations, the architecture of the data fusion algorithm results as in **Figure 3** [14]. The chosen fuzzy logic controllers are based on rules set that created

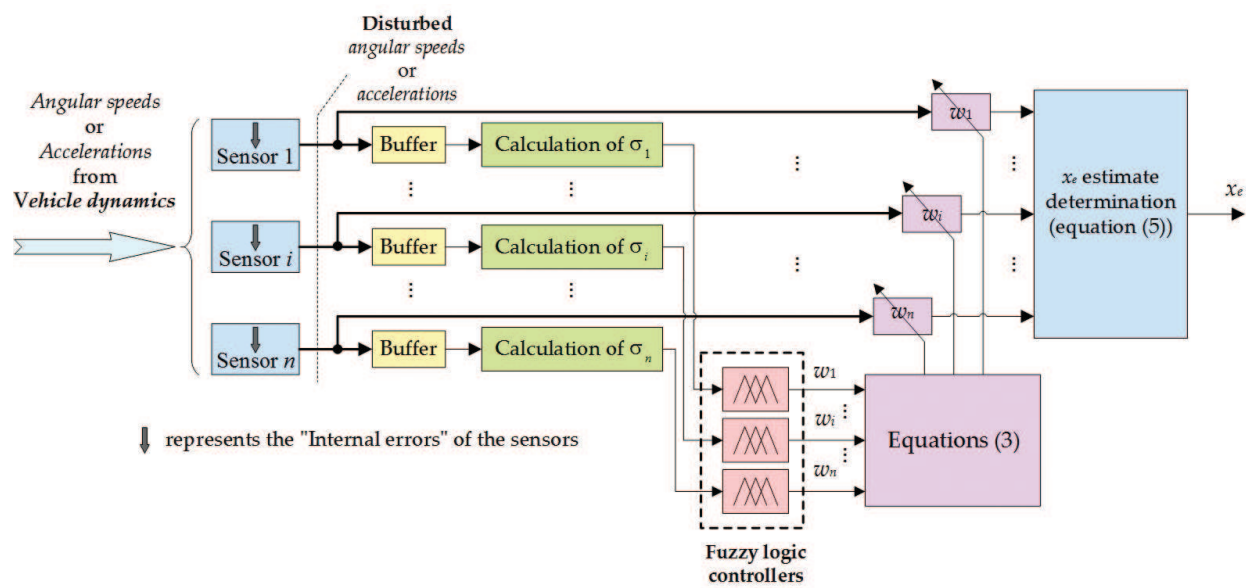


Figure 3. Data fusion algorithm.

a proportional dependence between the quality of the sensor signals and their associated weights, e.g., a “P” fuzzy logic controller. Therefore, the implemented fuzzy logic controllers established an inverse proportionality between the calculated standard deviations and sensor-associated weights.

The aim is to obtain a simpler fuzzy controller in order to reduce at minimum the computing time at each sample in order to implement the controller on a cheaper microcontroller. The way to reduce the computing time is to reduce on one hand the number of the membership functions and on the other hand to simplify these functions. The structure of fuzzy controller realized in Matlab/Simulink is presented in **Figure 4** [20, 21].

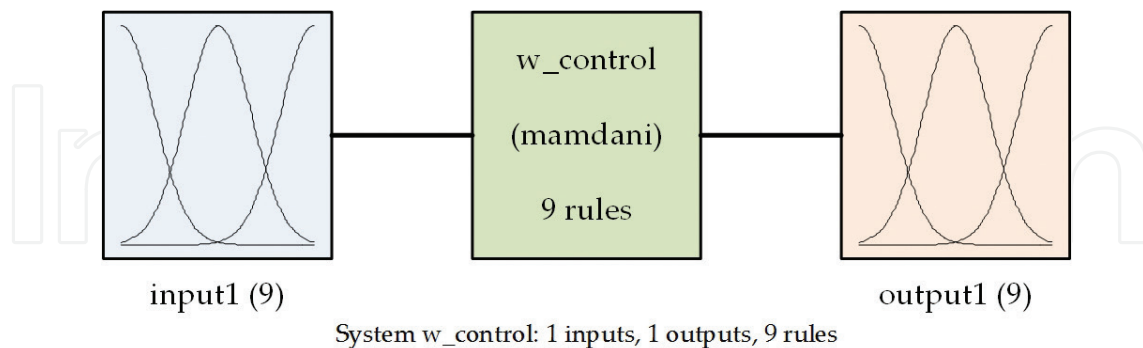


Figure 4. Fuzzy controller structure.

The universe of discourse for the controller input has considered a $[0, 2]$ interval, where nine membership functions (*in1* to *in9*) with Gaussian shapes were uniformly distributed. In the same time, nine membership functions (*out1* to *out9*) with similar shapes were considered in the $[0, 1]$ interval, taken as universe of discourse for the output. **Figure 5** presents the input/output membership functions.

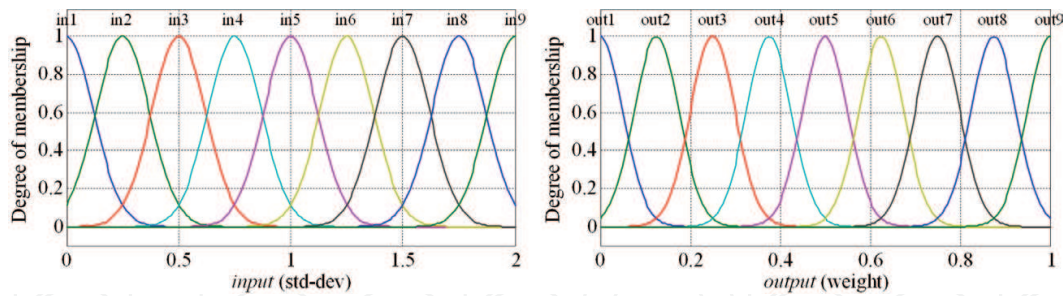


Figure 5. Membership functions (mfs) for input and output.

In the fuzzification process, the next nine rules were defined as: (1) If (*input* is *in1*) then (*output* is *out9*); (2) If (*input* is *in2*) then (*output* is *out8*); (3) If (*input* is *in3*) then (*output* is *out7*); (4) If (*input* is *in4*) then (*output* is *out6*); (5) If (*input* is *in5*) then (*output* is *out5*); (6) If (*input* is *in6*) then (*output* is *out4*); (7) If (*input* is *in7*) then (*output* is *out3*); (8) If (*input* is *in8*) then (*output* is *out2*); and (9) If (*input* is *in9*) then (*output* is *out1*). Widely accepted for capturing expert knowledge, a Mamdani controller type was used due to its simple structure of “min-max” operations [21]; and for defuzzification, the centroid method was applied.

3. Numerical simulation results

To simulate the algorithm, some models in Matlab/Simulink for detection clusters with various sizes and sensors types were realized. An example of such model is shown in **Figure 6**, being realized for a cluster with four sensors by the same type, with errors software modeled by the blocks “Model Acc” placed at the input of the simulation model. These models, realized by the authors, are based on the sensor data sheets and on the IEEE equivalent models for the inertial sensors [22, 23]. Accelerometers were modeled as in **Figure 7**, the obtained model having inputs, such as acceleration a_x , applied along the sensitive axis, and the cross-axis acceleration a_y , and as output the perturbed acceleration a [22, 23].

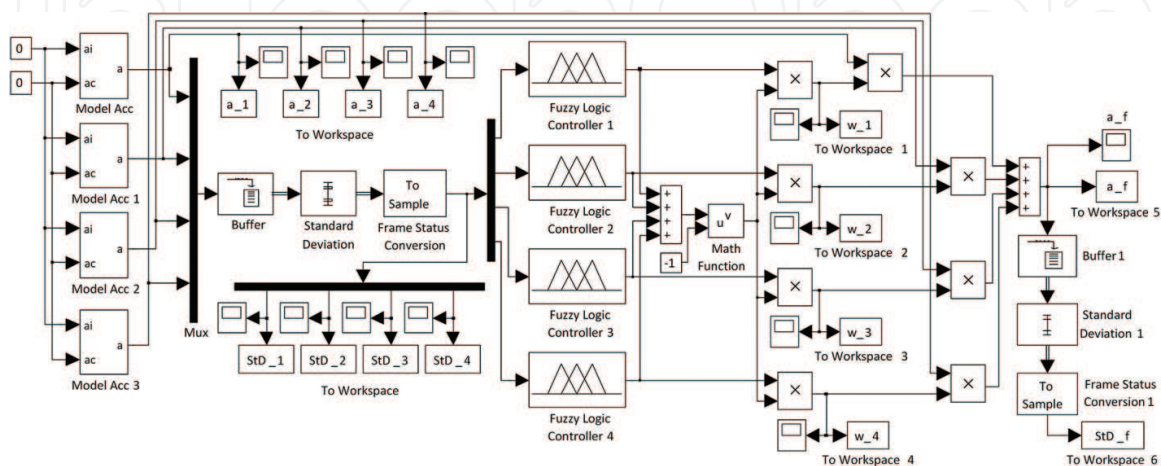


Figure 6. Simulation model with four sensors in cluster.

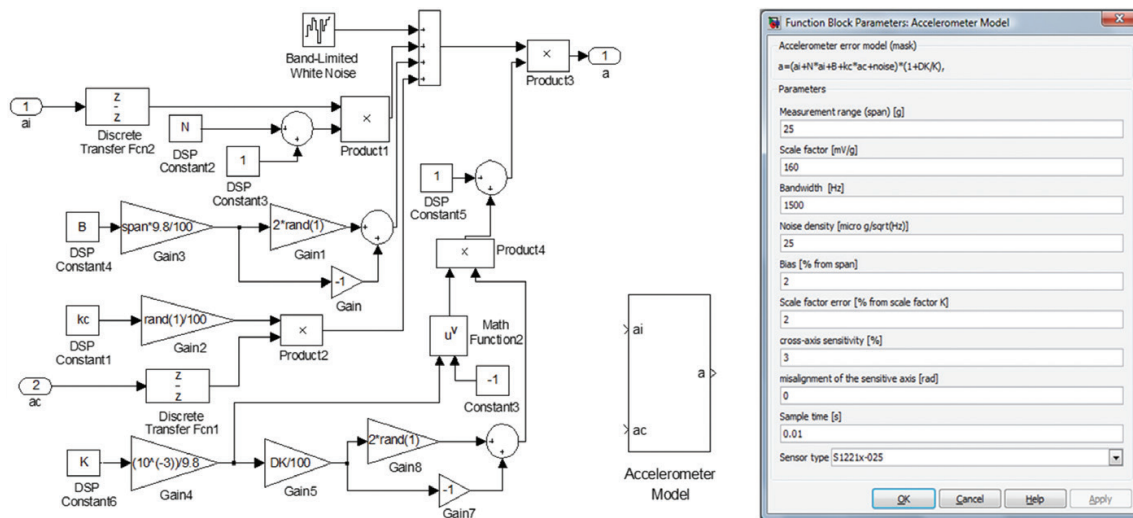


Figure 7. Accelerometers Matlab/Simulink model and its interface.

Studying the data sheets for various acceleration sensors, it was observed that a part of the included parameters is provided by using an interval inside which they can vary arbitrary. For example, for the bias it is provided a maximum absolute value (B) which is considered as percent from span, for the cross-axis sensitivity it is provided a maximal value (k_c) considered as a percent from the cross-axis acceleration (a_c), for the scale factor calibration error the producers give a maximum absolute value (ΔK) under the form of a percent from the scale factor (K), and for the noise is provided the maximum value of its density. Therefore, according to **Figure 7**, in the model, the “rand(1)” MATLAB function is used three times to generate a random value in the $(-B, B)$ interval for the bias, a random value in the $(0, k_c)$ interval for the cross-axis sensitivity, and a random value in the $(-\Delta K, \Delta K)$ interval for the scale factor calibration error. The noises are realized using the SIMULINK block “Band-Limited White Noise” and MATLAB function “RandSeed” through the generation of a random value of the density in the $(80\% \cdot v_d, v_d)$ interval [24].

In a simulation example at null accelerations as inputs, graphical characteristics resulted are shown in **Figures 8–10**. **Figure 8** shows the sensor measurements from “Acc-1” to “Acc-4” and also the results of the accelerometer data fusion “Acc-f”. In the simulation, there was considered just the sensor noise overlapped on an ideal null input for four sensors with a span of 18 g, a bandwidth of 2500 Hz each, and with various noise densities taken aleatory between 280 and 380 $\mu\text{g}/\text{Hz}^{1/2}$. The noise pattern of the data fusion resulted a signal that proves an important reduction of the noise level, a similar observation resulting from **Figure 9** also depicting the evolution in time of the standard deviations for the sensors signals and for the estimate x_e . On the other way, **Figure 9** proves that the adaptive character of the algorithm is maintained, the standard deviations values being updated at each simulation time step. The best sensor in the cluster was sensor #3, the standard deviation of the fused signal being two times smaller (approx. $3 \cdot 10^{-3} \text{ m/s}^2$) than the raw values of the standard deviations of the sensors signals (approx. $6 \cdot 10^{-3} \text{ m/s}^2$). **Figure 10**, depicting the values of the sensor weights estimated at each calculation step, also proves that the best sensor in the cluster was the sensor #3, and it receives the biggest values from the four weights during the entire numerical simulation.

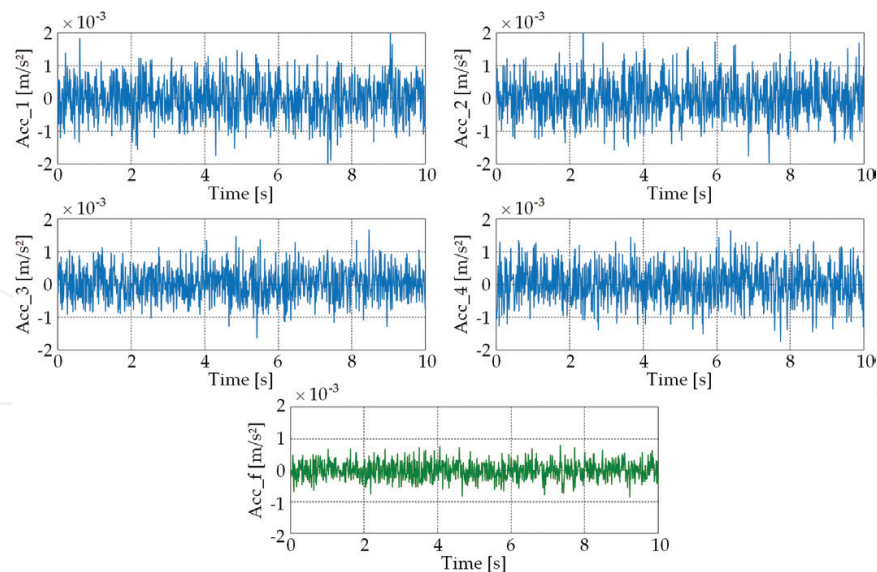


Figure 8. The sensor measurements and the data fusion results.

The sample time for the numerical simulation was 0.01 s, which means a data processing rate of 100 samples/s. Moreover, the data frame size for one detection channel was established to be $m = 100$, i.e., the buffers allow to be obtained data frames of 100 consecutive samples for each channel. In this way, any two consecutive data frames for one channel are overlapped with 99 samples. From **Figure 9**, the initialization phase of the algorithm with a duration of 1 s, time necessary for the first buffer to be full with 100 samples can be easily observed. All simulation results proved a good functioning of the algorithm which provided an important reduction of the sensor noise level, with a higher potential in the improvement of the solution of navigation accuracy when it is used in an inertial navigator.

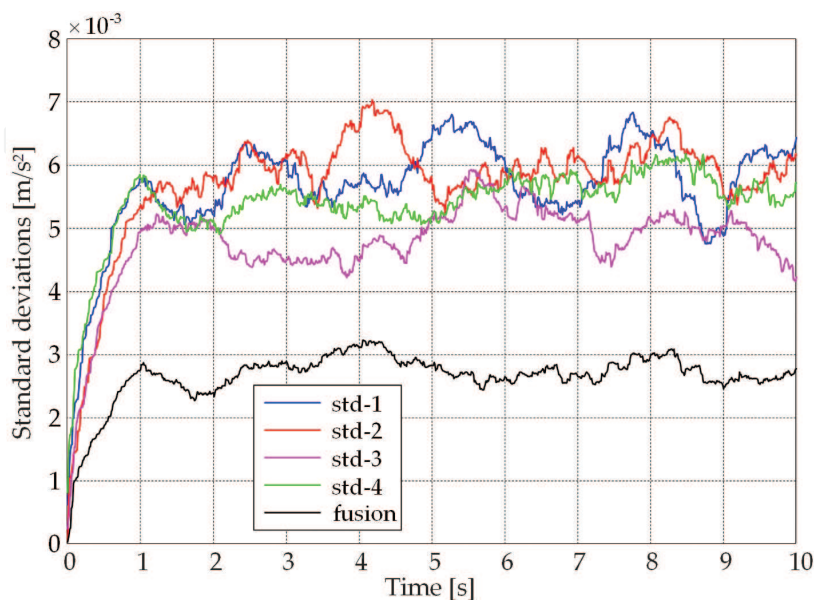


Figure 9. Standard deviations for the sensor signals and for the data fusion signals.

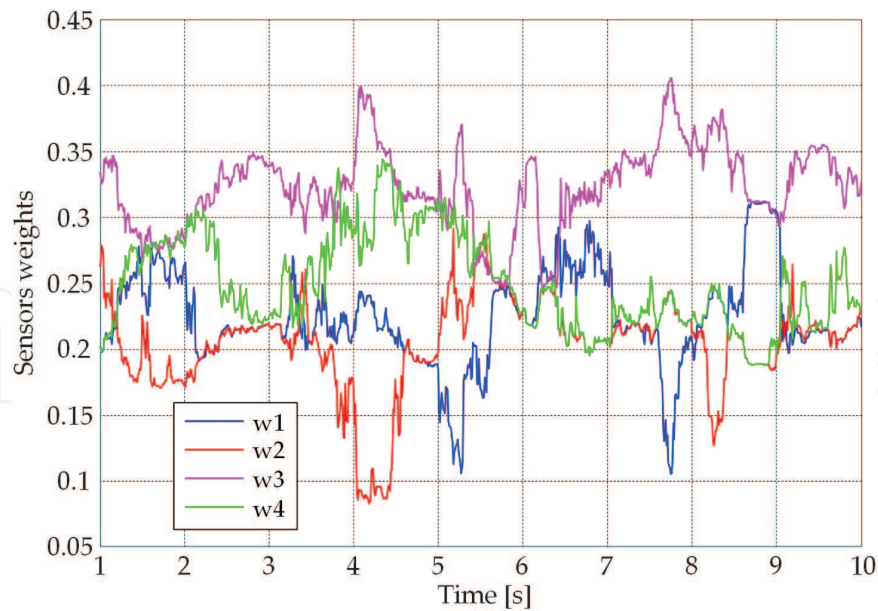


Figure 10. Sensor weights.

4. Results obtained with experimental data

The proposed algorithm was also tested using some experimental data acquired with an IMU equipped with detection clusters, which included six MEMS sensors each (assisted by an integrated GPS/INS navigator as reference positioning system). For the used IMU structure, with six sensors in each detection cluster, the Matlab/Simulink implementation of the data fusion algorithm resulted as shown in **Figure 11** [14]. Grouping the algorithm model resulted in “Fuzzy-logic data fusion” block from the right side of the figure. The data fusion block inputs are the measured data obtained from the sensors in the cluster (“Si” correspond to the

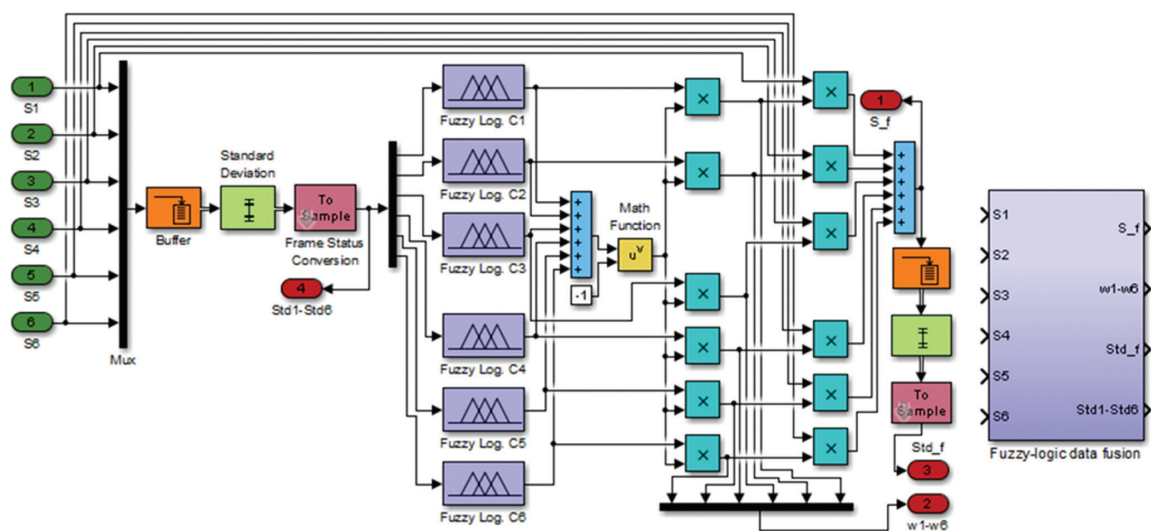


Figure 11. Matlab/Simulink implementation of the data fusion algorithm for experimental data.

measurements x_i , $i = 1 \div 6$), whereas its outputs are the fusion signal “S_f” (the estimate x_e), the sensor weights “w1–w6” (w_i , $i = 1 \div 6$), the standard deviation of the fusion signal “Std_f”, and the standard deviations of the sensor data “Std1–Std6”.

After the fusion, the obtained data were processed in a bidimensional INS navigator in horizontal plane, software implemented as in **Figure 12** [14]. Therefore, in this testing mechanism, three detection clusters were implied: two accelerometers clusters along the longitudinal and lateral axes of the vehicle and a gyro cluster along the vertical axis of the vehicle. The model included the “Flat Earth to LLA” Matlab/Simulink block in order to obtain the vehicle coordinates also in terms of latitude and longitude. The block “Horizontal plane navigator” in the right side of the figure has been obtained by grouping the navigator software model in the left side of the figure. The inputs of the navigator are the inertial measurements provided by the accelerometers and by the gyro: longitudinal (f_{xv}) and lateral (f_{yv}) accelerations in vehicle reference frame, and the angular speed (w_{zv}) along the vertical axis of the vehicle reference frame. As outputs, it provides information related to the angular orientation of the vehicle in horizontal plane (yaw angle— ψ), to the vehicle speed and position components in local horizontal frame, v_{xl} (North speed), v_{yl} (East speed), x_l (position in North direction), and y_l (position in East direction), and to the latitude and longitude coordinates of the vehicle (Lat and Lon).

During tests, the IMU data were acquired simultaneously with the data from an integrated GPS/INS navigator used as reference positioning system; both equipments were boarded on a test car. The sensor acquired data were offline processed through fusion but also used together with the fusion signals in a Matlab/Simulink software model implementing seven bidimensional INS navigators (“Horizontal plane navigator” blocks) as in **Figure 13** [14]. It also includes three “Fuzzy-logic data fusion” blocks used to fuse the acquired data in each of the three detection clusters.

The sensors in IMU were organized in six groups, with three sensors each (two accelerometers and one gyro), one sensor from each of the three detection clusters. To avoid the complications in the data processing, the detection groups included sensors with the same number in

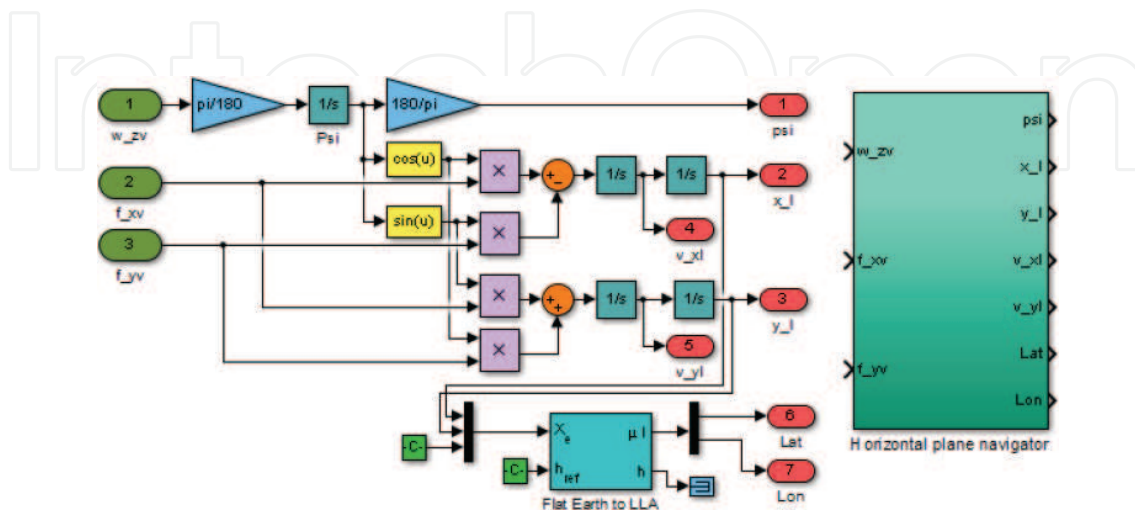


Figure 12. Software model of the bidimensional INS navigator in horizontal plane.

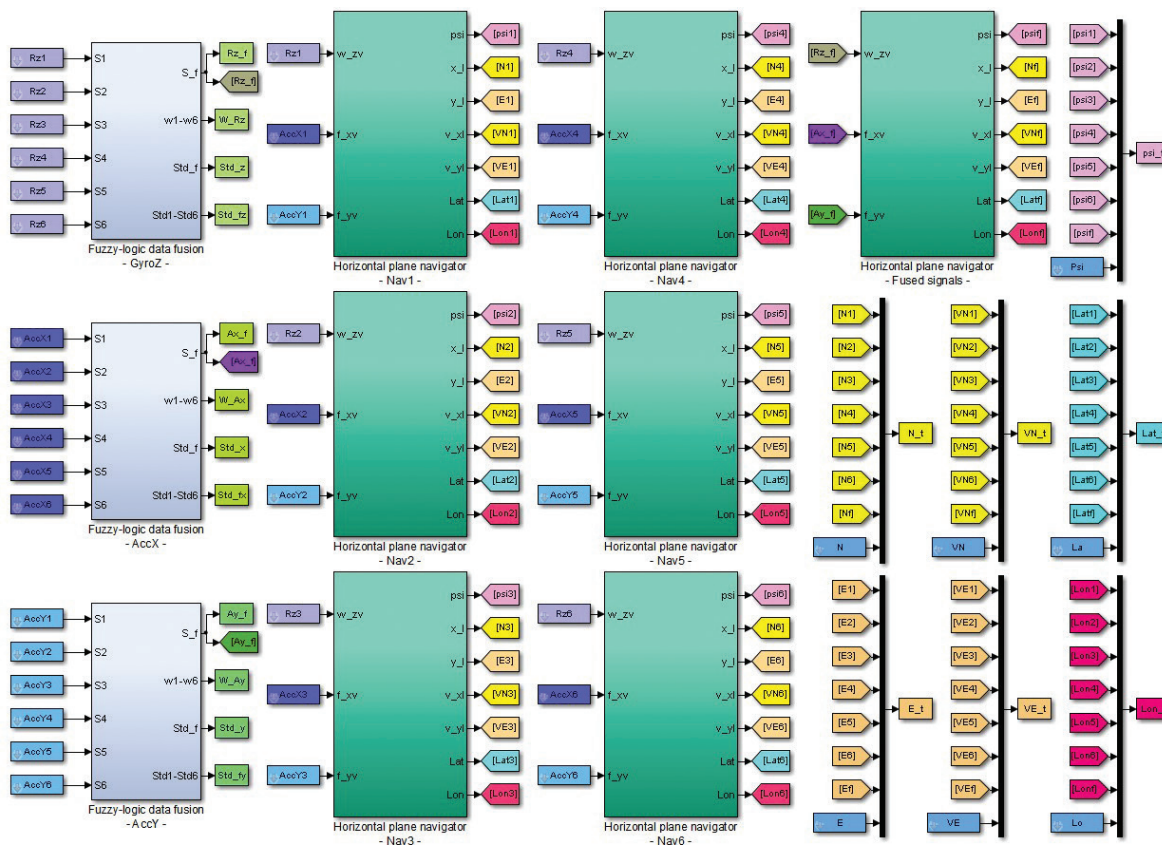


Figure 13. The evaluation Matlab/Simulink model.

the detection clusters. Six of the seven navigators in **Figure 13** (“Nav1” to “Nav6”) processed data from the six detection groups, whereas the seventh navigator (“Horizontal plane navigator – Fused signals”) processed data resulted from the fusion procedure applied on each of the three detection clusters. In this way, the evaluation model allows the obtaining of seven solutions of navigation, six solutions based on inertial sensor raw data (nonredundant INSs) and one solution based on inertial sensor fused data. All these solutions are further compared with the navigation solution provided by the integrated GPS/INS navigators which are used as reference positioning system.

For an evaluation situation, the experimental data acquired in each of the three detection clusters and the data fusion results for each cluster are shown in **Figure 14** for the accelerometers in the x -axis cluster, in **Figure 15** for the accelerometers in the y -axis cluster, and in **Figure 16** for the gyros in z -axis cluster. The data fusion signals are the last ones in each figure.

The processing of the acquired data with the model in **Figure 13** conducted at the navigation solutions components shown in the next figures. Together with the navigation solution, components have shown the associated errors, evaluated vis-à-vis of the reference navigation solution provided by the GPS/INS integrated navigator. **Table 1** centralizes the absolute maximal values of the positioning and speed errors for all six nonredundant INSs (“INS1” to “INS6” columns) and for the redundant INS (“Fusion” column), and also the mean values obtained for all these errors (“Mean value” column). In the same time, by calculating the mean

of the absolute maximal values of the errors for the six nonredundant INSs in each line of **Table 1** and dividing it with the corresponding value in the “Fusion” column, the ratios in the “Mean/Fus” column have been obtained. Similarly, the “Max/Fus” and “Min/Fus” columns show the ratios between the maximal value of the tabled errors for the six nonredundant INSs in each line of **Table 1** and the corresponding value in the “Fusion” column, respectively, between the minimum value of the tabled errors for the six nonredundant INSs in each line of **Table 1** and the corresponding value in the “Fusion” column.

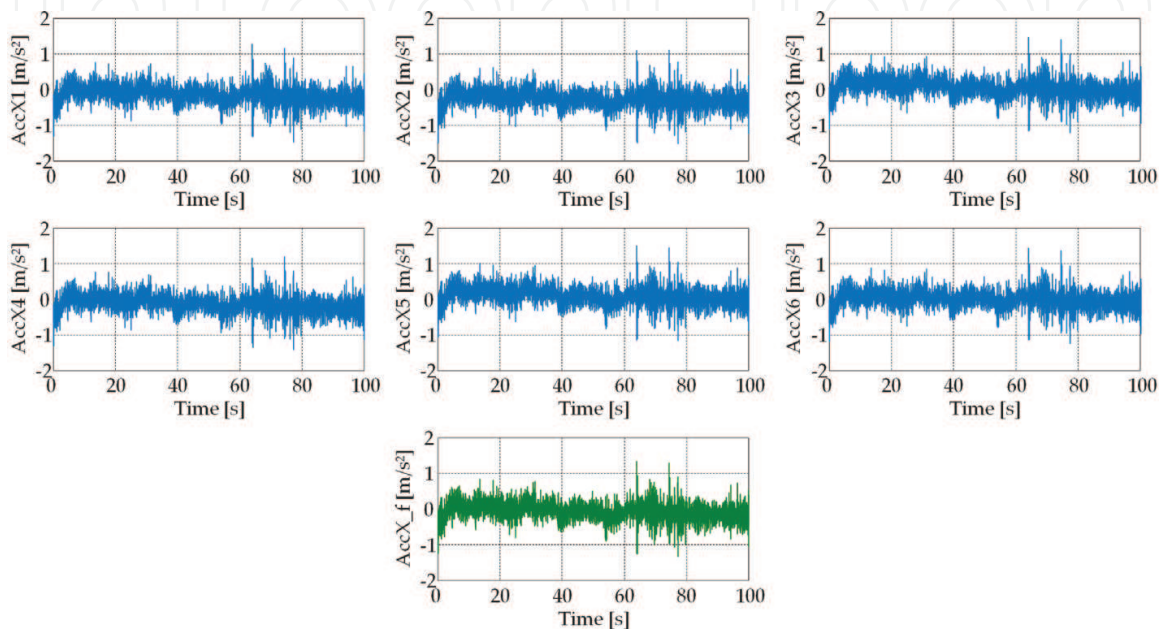


Figure 14. Experimental data and the data fusion results for accelerometers in the x -axis cluster.

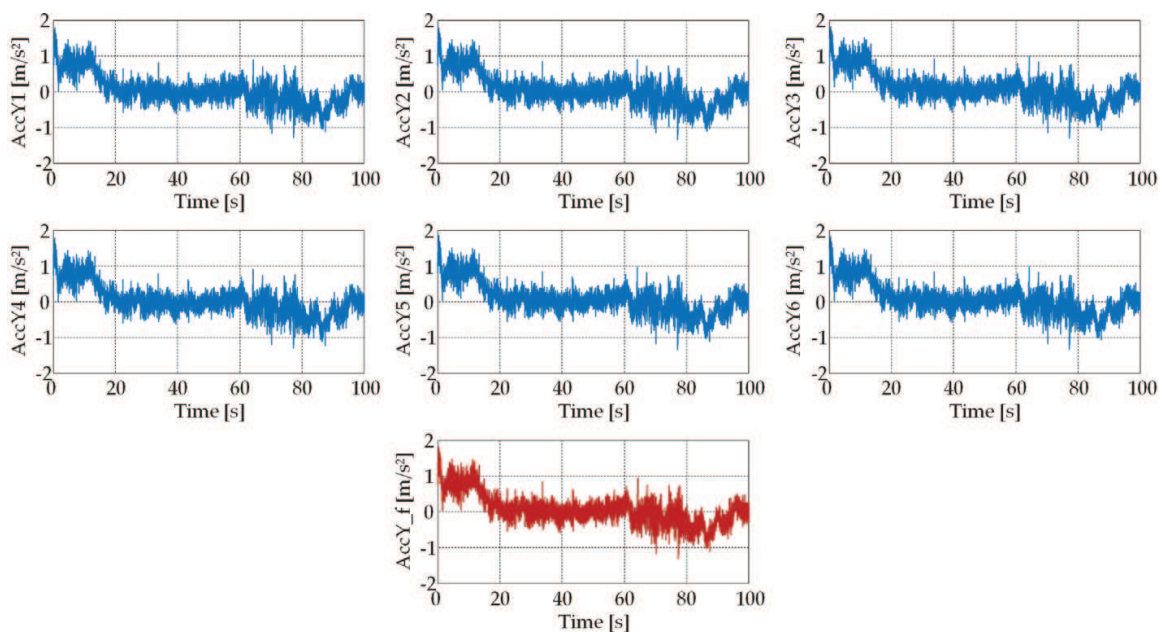


Figure 15. Experimental data and the data fusion results for gyros in the z axis cluster.

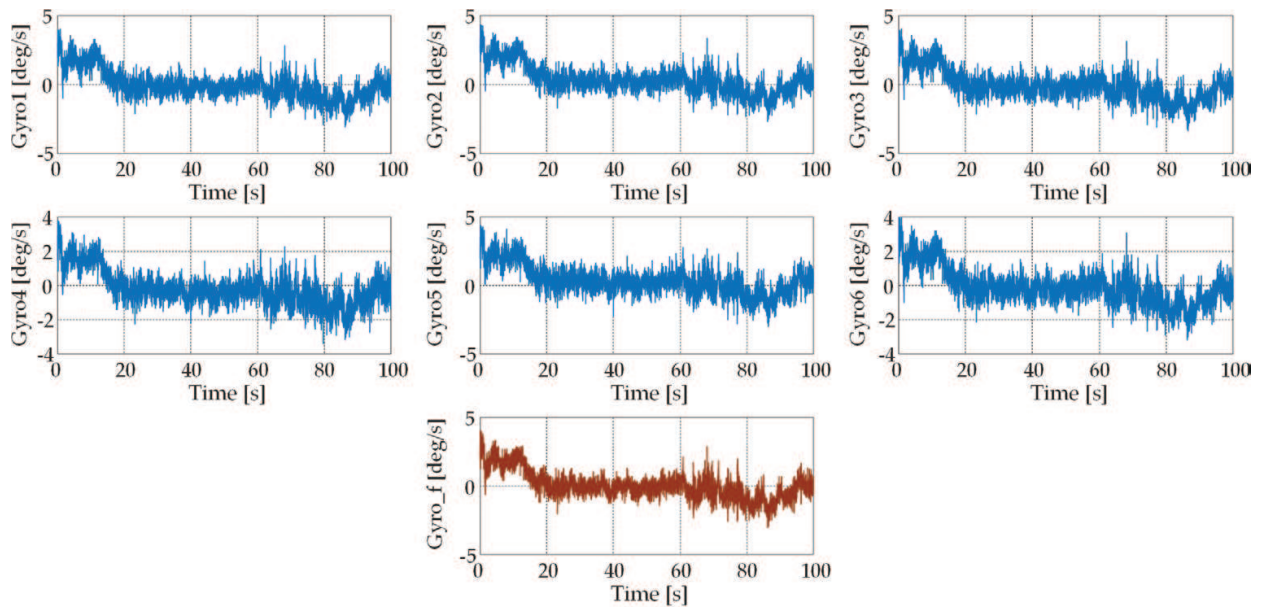


Figure 16. Experimental data and the data fusion results for gyros in the z axis cluster.

At the level of the vehicle attitude, the characteristics in **Figure 17** were obtained for the yaw angle. Also, from the point of view of the horizontal positioning, **Figure 18** presents the covered distances in the North direction, and **Figure 19** presents the covered distances in East direction. The North speed evolutions during time are depicted in **Figure 20**, whereas the speed evolutions during time in the East direction are shown in **Figure 21**. For each navigator, the incorporated “Flat Earth to LLA” block allows the calculus of the vehicle Latitude and Longitude as shown in **Figures 22** and **23**. Combining the positioning data in a horizontal plane, it resulted the vehicle trajectories (Latitude versus Longitude) and the deviations from the reference trajectory (Latitude errors versus Longitude errors), established by all seven navigators, as in **Figure 24**.

Figure 25 depicts the time evolution of the vehicle trajectories estimated with all seven navigators, whereas **Figure 26** presents their deviations from the reference trajectory.

Both graphical results and numerical values presented in **Table 1** prove an important positioning precision improvement by using the proposed data fusion mechanism. The errors of the navigation solution are substantially reduced comparatively with the nonredundant navigation solutions. The numerical data in the “Mean/Fus” column of **Table 1** highlighted a decrease of the mean of the absolute maximal values of the errors for the six nonredundant INSs of approximately 16.6 times for the positioning in the North direction, 5.1 times for the positioning in the East direction, 2.8 times for the speed component in North direction, 1.05 times for the speed component in the East direction, and 3.8 times in the angular positioning in the horizontal plane (yaw angle). It is very important to be mentioned that the inertial sensor outputs in the experimental model of the inertial measurement unit were not previously corrected with the biases values or with other errors values. The values in the “Fusion” column of **Table 1**, related to the positioning and speed errors for the redundant navigator after 100 s have shown us that the absolute maximal values of these errors were 32.67 m for the linear

Abs. max error	INS1	INS2	INS3	INS4	INS5	INS6	Fusion	Mean value	Mean/Fus	Max/Fus	Min/Fus
North [m]	411.3583	990.5235	599.5493	308.5221	692.1193	266.7808	32.6736	544.8089	16.6742	30.3156	8.1650
East [m]	73.0415	318.1701	262.5502	107.2303	310.4679	132.3827	39.2776	200.6405	5.1082	8.1005	1.8596
V-North [m/s]	9.0599	19.4083	11.1598	7.1313	14.0987	7.0160	4.0333	11.3123	2.8046	4.8119	1.7395
V-East [m/s]	10.9701	9.8672	3.4987	13.6819	1.5752	5.5067	7.1445	7.5166	1.0520	1.9150	0.2204
Latitude [degrees]	$37.019 \cdot 10^{-4}$	$89.141 \cdot 10^{-4}$	$53.955 \cdot 10^{-4}$	$27.765 \cdot 10^{-4}$	$62.286 \cdot 10^{-4}$	$24.008 \cdot 10^{-4}$	$2.940 \cdot 10^{-4}$	$49.029 \cdot 10^{-4}$	16.6742	30.3156	8.1659
Longitude [degrees]	$9.156 \cdot 10^{-4}$	$39.886 \cdot 10^{-4}$	$32.914 \cdot 10^{-4}$	$13.442 \cdot 10^{-4}$	$38.921 \cdot 10^{-4}$	$16.595 \cdot 10^{-4}$	$4.923 \cdot 10^{-4}$	$25.152 \cdot 10^{-4}$	5.1082	8.1005	1.8598
Yaw [degrees]	14.4621	25.2716	18.7894	31.1004	24.9227	19.4309	5.7402	22.3295	3.8899	5.4179	2.5194

Table 1. Error analysis for redundant INS and for nonredundant INSs.

positioning in North direction, 39.27 m for the linear positioning in East direction, 2.03 m/s for the speed component in North direction, 7.14 m/s for the speed component in East direction, $2.940 \cdot 10^{-4}$ degrees for the Latitude positioning, $4.923 \cdot 10^{-4}$ degrees for the Longitude positioning, and 5.74 degrees for the angular positioning in the horizontal plane (Yaw angle).

The nonredundant inertial navigation system’s best configuration was switched between the detection groups associated with the first sensor in each detection cluster (East channel and Yaw angle channel) and with the sixth sensor in each detection cluster (North channel). The worst configurations for the nonredundant INSs are for the second sensor in each detection cluster, the absolute maximal values of errors in North position channel being 990.52 m, 318.17 m in East position channel, 19.40 m/s in North speed channel, $89.141 \cdot 10^{-4}$ degrees in the Latitude position channel, and $39.886 \cdot 10^{-4}$ degrees in the Longitude channel. From the point of view of East speed channel and yaw angle channel, the worst nonredundant INS is INS4, the East speed error being 13.68 m/s and the yaw angle error being 31.10 degrees.

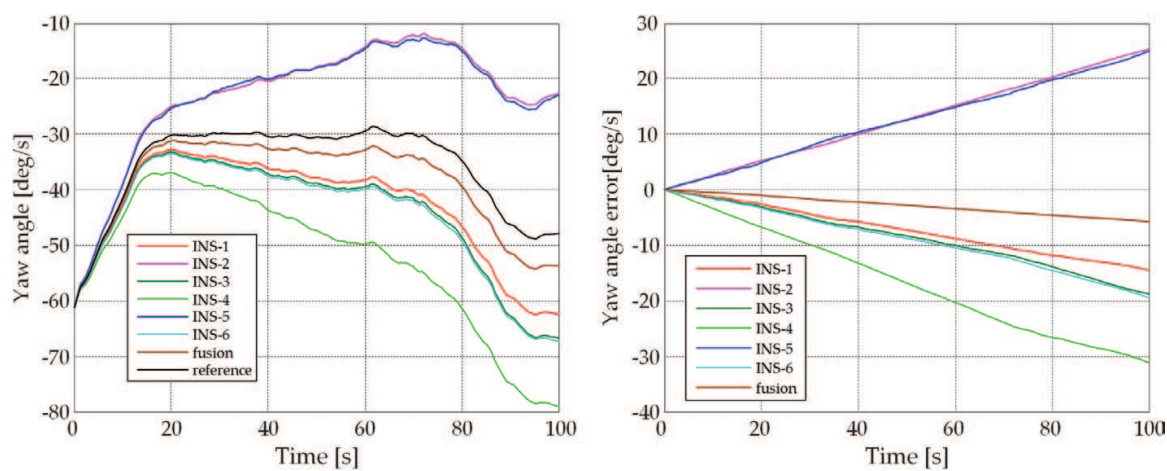


Figure 17. Yaw angle values and errors.

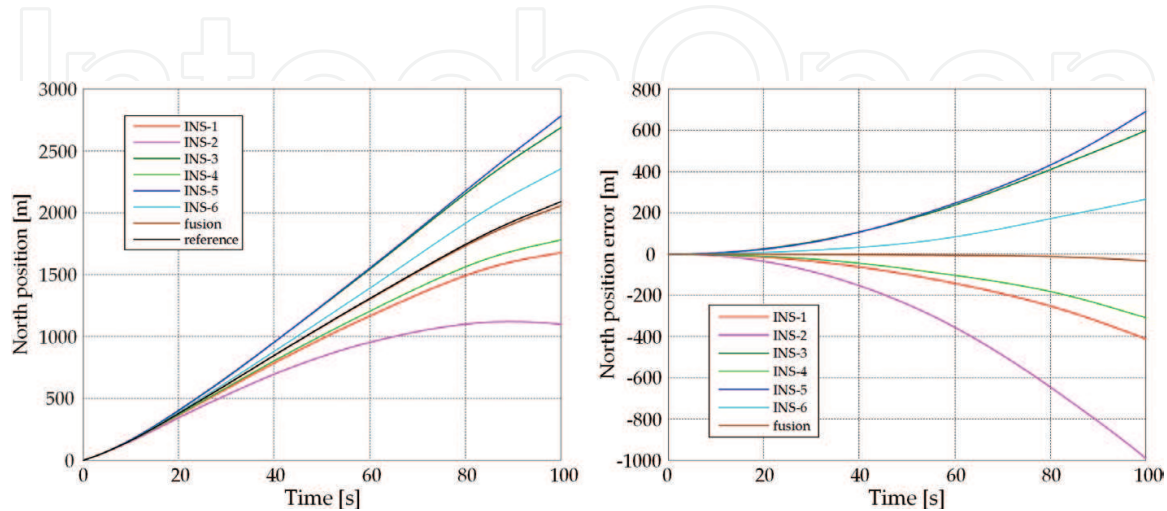


Figure 18. North positions and errors.

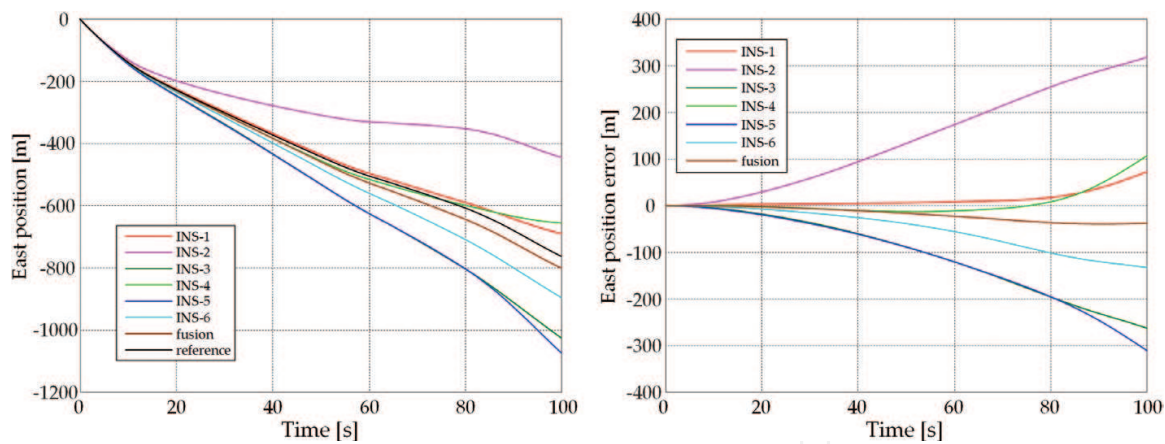


Figure 19. East positions and errors.

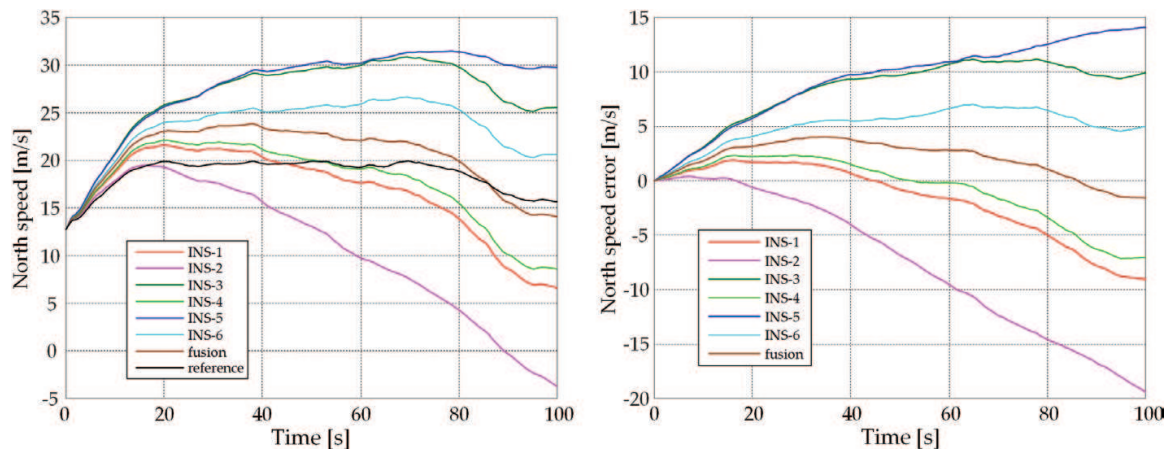


Figure 20. North speed evolutions during time.

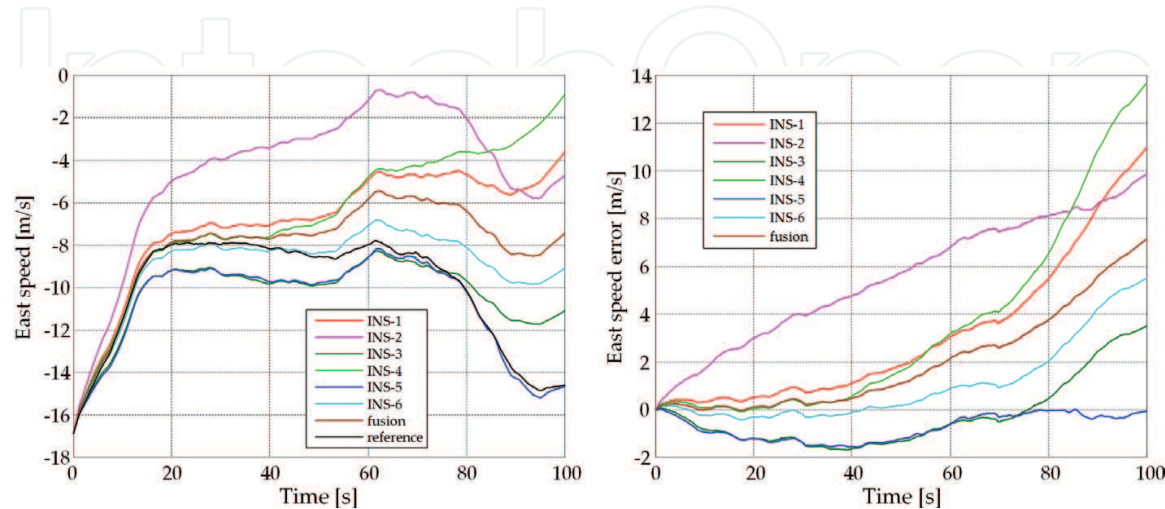


Figure 21. East speed evolutions during time.

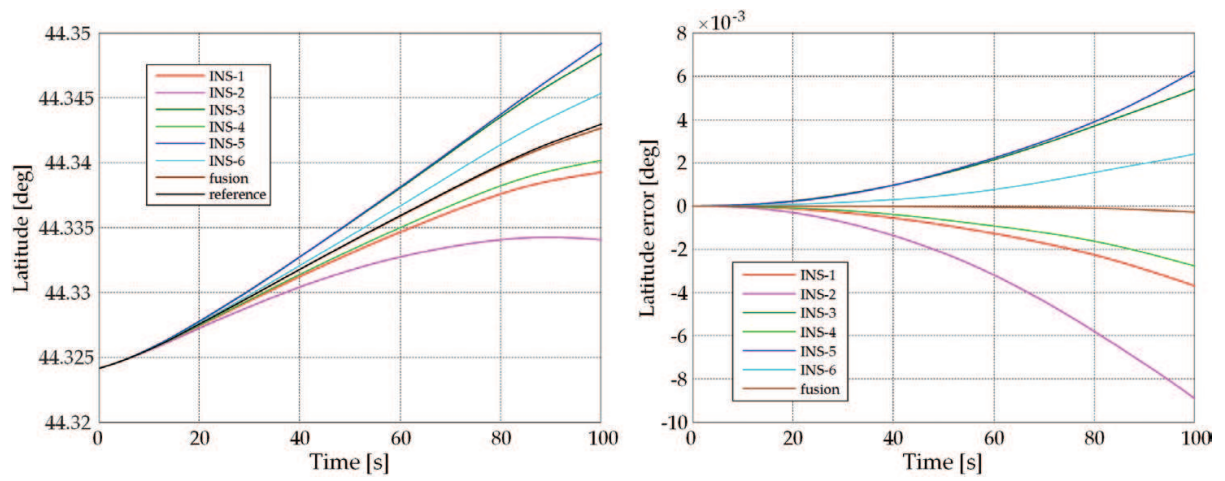


Figure 22. Latitude and errors.

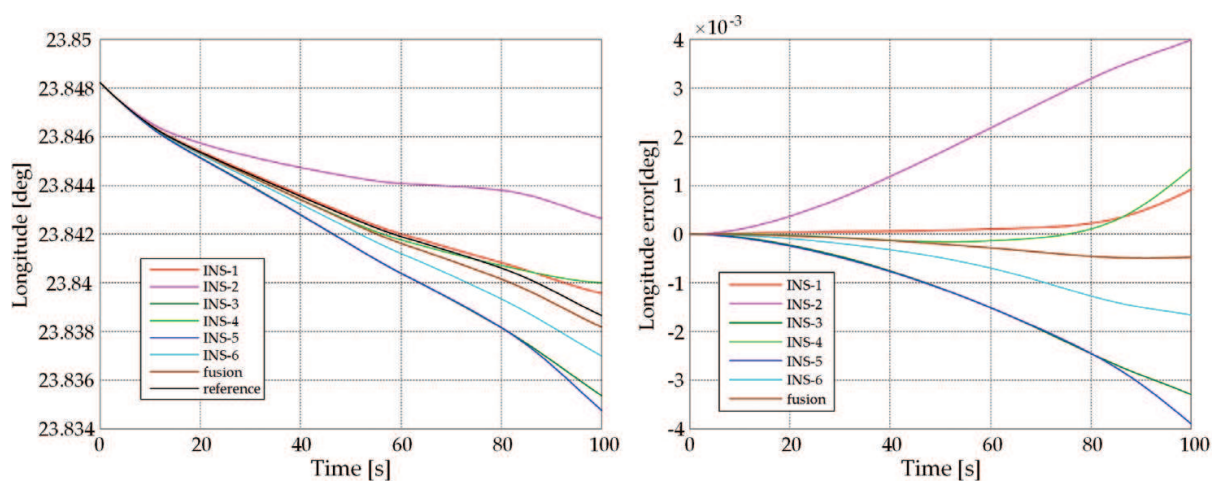


Figure 23. Longitude and errors.

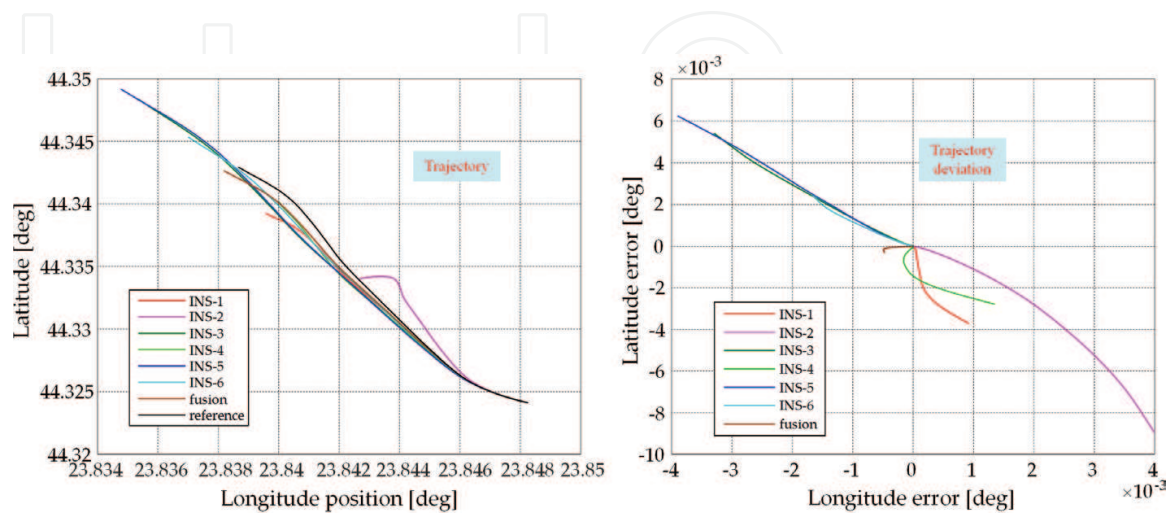


Figure 24. Vehicle trajectories and deviations from the reference trajectory in horizontal plane.

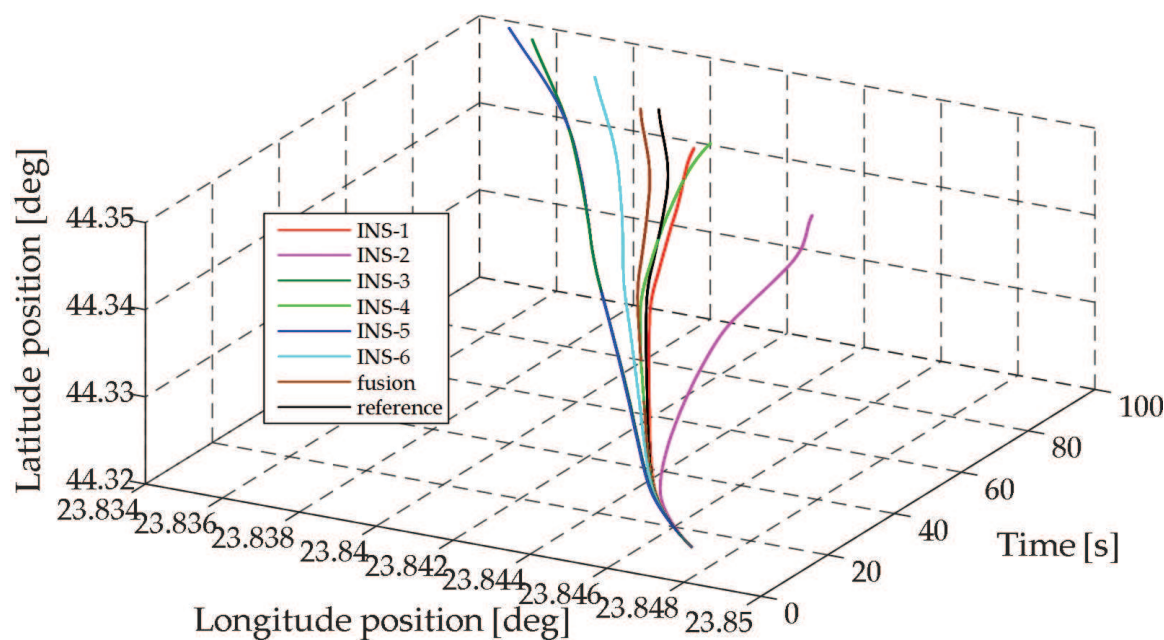


Figure 25. The time evolution of the vehicle trajectories for all seven INSs.

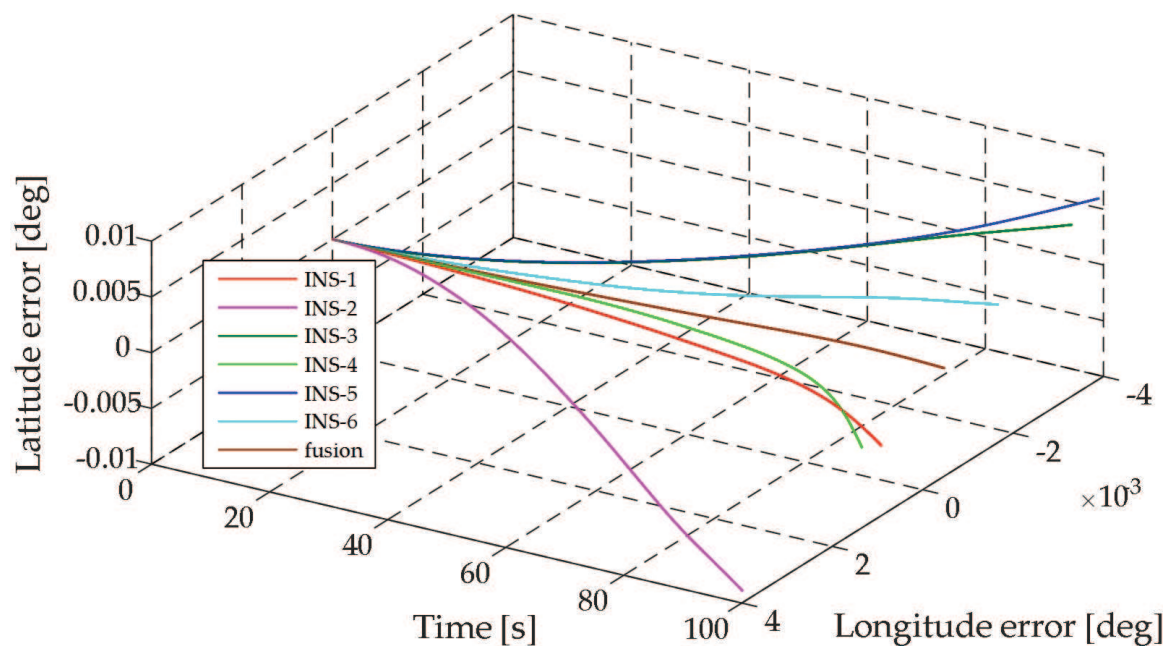


Figure 26. Time evolution of the deviations of the vehicle from the reference trajectory.

5. Conclusions

The chapter exposed a new way to reduce the noise in the inertial sensor data based on a fuzzy logic mechanism. As a special need of the developed mechanism is considered to be a redundant inertial measurement unit with inertial sensors disposed in detection clusters

with linear configurations, and measuring the same quantity. The proposed algorithm was firstly numerically simulated based on some models in Matlab/Simulink realized for detection of clusters with various sizes and including various sensor types. All simulation results proved a good functioning of the algorithm which provided an important reduction of the sensor noise level, with a higher potential in the improvement of the solution of navigation accuracy when it is used in an inertial navigator. Second, the algorithm was integrated in an INS redundant structure, with an IMU with three detection clusters and six miniaturized sensors in each cluster. An integrated GPS/INS navigator was used as reference positioning system to estimate the errors of the redundant INS in each channel of the solution of navigation. The data acquired from the redundant IMU were used in a software model both in nonredundant configuration, to compute the solutions of navigations for six detection groups which included sensors with the same number in the detection clusters, but also for the INS redundant configuration when our data fusion methodology is preliminary applied. Both graphical results and tabled numerical values proved an important positioning precision improvement by using the proposed data fusion mechanism. The errors of the navigation solution were substantially reduced comparatively with the nonredundant navigation solutions. The numerical data highlighted a decrease of the mean of the absolute maximal values of the errors for the six nonredundant INSs of approximately 16.6 times for the positioning in the North direction, 5.1 times for the positioning in the East direction, 2.8 times for the speed component in North direction, 1.05 times for the speed component in the East direction, and 3.8 times in the angular positioning in the horizontal plane (yaw angle). It is very important to be mentioned that the inertial sensor outputs in the experimental model of the inertial measurement unit were not previously corrected with the biased values or with other errors values.

Acknowledgements

This work was supported by the CNCSIS-UEFISCSU, project PN II-RU, No. 1/28.07.2010, "High-precision strap-down inertial navigators, based on the connection and adaptive integration of the nano and micro inertial sensors in low cost networks, with a high degree of redundancy," code TE-102/2010.

Author details

Teodor Lucian Grigorie^{1*} and Ruxandra Mihaela Botez²

*Address all correspondence to: ltgrigorie@yahoo.com

¹ University of Craiova, Craiova, Romania

² École de Technologie Supérieure, Montréal, Canada

References

- [1] Barbour, N.M. Inertial navigation sensors. In: NATO RTO-EN-SET-116; 2010.
- [2] Barbour, N.M., Schmidt, G. Inertial sensor technology trends. *IEEE Sensors Journal*. 2001;1(4):332-339.
- [3] Barbour, N.M. et al. Inertial MEMS Systems and Applications. In: NATO RTO-EN-SET-116-2011, Low-Cost Navigation Sensors and Integration Technology; Bagneux, France, 28-29 March, 2011.
- [4] Schmidt, G.T. INS/GPS technology trends. In: NATO RTO-EN-SET-116-2011, Low-Cost Navigation Sensors and Integration Technology; Bagneux, France, 28-29 March, 2011.
- [5] Farrell, J. Aided Navigation. GPS with High Rate Sensors. McGraw-Hill, New York; 2008.
- [6] Mohinder, S., Lawrence, R., Angus, P. Global Positioning Systems, Inertial Navigation, and Integration. John Wiley & Sons, Inc., Hoboken, New Jersey, 2001.
- [7] Titterton, D.H., Weston, J. Strapdown Inertial Navigation Technology. 2nd ed. IET, Stevenage Herts, United Kingdom; 2004.
- [8] Grigorie, T.L., Sandu, D.G. Navigation Systems Synergic Architectures With Strap-Down Inertial Components. SITECH, Craiova, Romania; 2013.
- [9] Grigorie, T.L., Edu, I.R. Inertial Navigation Applications With Miniaturized Sensors. SITECH, Craiova, Romania; 2013.
- [10] He, X., Hu, X., Wu, M. Trends in GNSS/INS Integrated Navigation Technology. *Coordinates*. 2007; III(3):26-28.
- [11] Al-Faiz, M.Z., Ismaeel, S.A. Design of Kalman filter for augmenting GPS to INS systems. In: International Conference on Advanced Remote Sensing for Earth Observation. 2005; 14-20.
- [12] Lorinda, S., Aboelmagd, N. Bridging GPS outages using neural network estimates of ins position and velocity errors. *Measurement of Science & Technology*. 2006; 17:2783-2798.
- [13] Grigorie, T.L., Edu, I.R., Corcau, J.I. Fuzzy logic denoising of the miniaturized inertial sensors in redundant configurations. In: 33rd International Conference on Information Technology Interfaces (ITI 2011); June 27-30; Cavtat, Croatia. 2011. p. 521-526.
- [14] Grigorie, T.L., Botez, R.M. Positioning monitoring improvement in a horizontal plane ins by using fuzzy logic data fusion for denoising of inertial sensors in redundant clusters. *International Journal of Fuzzy Systems And Advanced Applications*. 2015; 2:33-40.

- [15] Hasan, A.M., Samsudin, K., Ramli, A.R., Azmir, R.S. Wavelet-based pre-filtering for low cost inertial sensors. *Journal of Applied Science*. 2010;10:2217-2230.
- [16] Mao, B., Wu, J.W., Wu, J.T., Zhou, X.M. MEMS gyro denoising based on second generation wavelet transform. In: *First International Conference on Pervasive Computing; China*. 2010. pp. 255-258.
- [17] Sabat, S.L., Giribabu, N., Nayak, J., Krishnaprasad, K. Characterization of fiber optics gyro and noise compensation using discrete wavelet transform. In: *Second International Conference on Emerging Trends in Engineering & Technology; Indian*. 2009. pp. 909-913.
- [18] Skaloud, B., Bruton, A.M., Schwartz, K. Detection and filtering of short-term (1/F) noise in inertial sensors. *Journal of the Institute of Navigation*. 1999; 46(2):97-107.
- [19] Grigorie, T.L., Negrea, P., Edu, I.R., Adochiei, F.C. Assistive positioning system based inertial techniques and wavelet denoising. In: *8th International Conference on Pervasive Technologies Related to Assistive Environments (PETRA); July 1-3, 2015; Corfu, Greece*. 2015
- [20] Kovacic, Z., Bogdan, S. *Fuzzy Controller Design – Theory and Applications*. Taylor and Francis Group, USA; 2006.
- [21] Castellano, G., Fanelli, A.M., Mencar, C. Design of transparent mamdani fuzzy inference systems. In: *Design and Application of Hybrid Intelligent Systems*. IOS, Amsterdam; 2003. pp. 468-476.
- [22] Grigorie, T.L., Lungu, M., Edu, I.R., Obreja, R. Concepts for error modeling of miniature accelerometers used in inertial navigation systems. *Annals of the University of Craiova, Electrical Engineering Series*. 2010; 34:212-219.
- [23] Grigorie, T.L., Botez, R.M. Modelling and simulation based Matlab/Simulink of a strap-down inertial navigation system' errors due to the inertial sensors. In: Kelly Bennett, editor. *Matlab Applications for the Practical Engineer*. InTech, Rijeka, Croatia; 2014. p. 305-338. DOI: 10.5772/57583
- [24] Grigorie, T.L., Botez, R.M. Modeling and numerical simulation of an algorithm for the inertial sensors errors reduction and for the increase of the strap-down navigator redundancy degree in a low cost architecture. *Transactions of the Canadian Society of the Mechanical Engineering (CSME)*. 2010; 34(1):1-16.